Arabidopsis TAF15b Localizes to RNA Processing Bodies and Contributes to snc1 -Mediated Autoimmunity

Oliver X Dong, Louis-Valentin Méteignier, Melodie B Plourde, Bulbul Ahmed, Ming Wang, Cassandra Jensen, Hailing Jin, Peter Moffett, Xin Li, Hugo Germain

MPMI Vol. 29, No. 4, 2016, pp. 247–257. http://dx.doi.org/10.1094/MPMI-11-15-0246-R

e-Xtra*

Arabidopsis TAF15b Localizes to RNA Processing Bodies and Contributes to *snc1*-Mediated Autoimmunity

Oliver X. Dong,[1,2] Louis-Valentin Meteignier,[3] Melodie B. Plourde,[4,5] Bulbul Ahmed,[4,5] Ming Wang,[6] Cassandra Jensen,[2] Hailing Jin,[6] Peter Moffett,[3] Xin Li,[1,2] and Hugo Germain[4,5]

[1]Department of Botany, University of British Columbia, Vancouver, BC, V6T 1Z4, Canada; [2]Michael Smith Laboratories, University of British Columbia; [3]Department of Biology, Université de Sherbrooke, Sherbrooke, QC, J1K 2R1, Canada; [4]Department of Chemistry, Biochemistry and Physics, Université du Québec à Trois-Rivières, QC, G9A 5H7, Canada; [5]Groupe de Recherche en Biologie Végétale (GRBV), Université du Québec à Trois-Rivières; and [6]Department of Plant Pathology and Microbiology, Center for Plant Cell Biology, Institute for Integrative Genome Biology, University of California, Riverside, CA 92521, U.S.A.

Submitted 2 November 2015. Accepted 21 December 2015.

In both animals and plants, messenger (m)RNA export has been shown to contribute to immune response regulation. The *Arabidopsis* nuclear protein MOS11, along with the nucleoporins MOS3/Nup96/SAR3 and Nup160/SAR1 are components of the mRNA export machinery and contribute to immunity mediated by nucleotide binding leucine-rich repeat immune receptors (NLR). The human MOS11 ortholog CIP29 is part of a small protein complex with three additional members: the RNA helicase DDX39, ALY, and TAF15b. We systematically assessed the biological roles of the *Arabidopsis* homologs of these proteins in toll interleukin 1 receptor–type NLR (TNL)-mediated immunity using reverse genetics. Although mutations in *ALY* and *DDX39* did not result in obvious defects, *taf15b* mutation partially suppressed the autoimmune phenotypes of a gain-of-function *TNL* mutant, *snc1*. An additive effect on *snc1* suppression was observed in *mos11-1 taf15b snc1* triple mutant plants, suggesting that MOS11 and TAF15b have independent functions. TAF15b-GFP fusion protein, which fully complemented *taf15b* mutant phenotypes, localized to nuclei similarly to MOS11. However, it was also targeted to cytosolic granules identified as processing bodies. In addition, we observed no change in *SNC1* mRNA levels, whereas less SNC1 protein accumulated in *taf15b* mutant, suggesting that TAF15b contributes to SNC1 homeostasis through posttranscriptional mechanisms. In summary, this study highlights the importance of posttranscriptional RNA processing mediated by TAF15b in the regulation of TNL-mediated immunity.

The plant immune system relies, in large part, on two distinct but converging molecular recognition mechanisms. In the first, cell surface–localized pattern recognition receptors detect conserved molecular motifs presented by pathogens and induce a low amplitude defense response, termed pathogen-associated molecular pattern (PAMP)-triggered immunity (PTI) (Boller and Felix 2009; Jones and Dangl 2006; Zipfel 2008). Successful pathogens, in turn, produce effector proteins (or virulence factors) that target PTI elements to inhibit this response (Fontes et al. 2004; Xiang et al. 2008) or, alternatively, use its effectors to rewire the host defense mechanism (Caillaud et al. 2013). The second layer of the plant immune system consists of an arsenal of highly polymorphic intracellular receptors that, once activated, triggers a stronger defense response referred to as effector-triggered immunity, which often culminates in the death of the infected cell (Jones and Dangl 2006). These intracellular receptors, commonly referred to as resistance proteins, are typically composed of three domains: an amino terminal domain consisting of either of a coil-coil domain or a toll interleukin 1 receptor (TIR) domain, a central nucleotide binding (NB) domain, and a leucine-rich repeat (LRR) carboxyl terminal domain (Chisholm et al. 2006), although other configurations do exist in the plant kingdom (Collier and Moffett 2009; Germain and Séguin 2011; Li et al. 2015). Remarkably, these NB-LRR receptors (NLR) share significant sequence similarities with animal innate immunity receptors such as Nod proteins, although they were believed to be derived from convergent evolution (Ausubel 2005; Rairdan and Moffett 2007).

One such NLR protein is the TIR-type NLR (TNL) SNC1 (Li et al. 2001). A point mutation, changing a glutamate (E) to a lysine (K) in the linker region located between the NB and LRR domains of SNC1, renders the snc1 protein more stable and constitutively activates TNL-mediated immunity (Cheng et al. 2011; Zhang et al. 2003). The *snc1* mutant phenotypes resulting from this gain-of-function mutation include increased accumulation of the defense hormone salicylic acid (SA), constitutive expression of defense-marker pathogenesis-related (*PR*) genes, and enhanced resistance to the biotrophic oomycete pathogen *Hyaloperonospora arabidopsidis* Noco2 and to the hemibiotrophic bacterial pathogen *Pseudomonas syringae* pv. *maculicola* ES4326. The morphology of *snc1* plants is also drastically affected, resulting in severely stunted stature, dark green color, and twisted leaves. All of these features are common to plants with elevated SA levels and constitutive expression of *PR* genes (Bowling et al. 1994; Clarke et al. 1998). These autoimmune morphological features have enabled forward genetic screens to be performed to investigate the molecular events surrounding SNC1 activation and homeostasis control (Johnson et al. 2013; Monaghan et al. 2010). Previously identified genetic suppressors, termed *modifier of snc1* (*mos*) mutants, revealed three nucleocytoplasmic trafficking pathways affecting immunity: nuclear localization signal–mediated nuclear import (Palma et al. 2005), nuclear export signal–mediated nuclear export (Cheng et al. 2009), and messenger (m)RNA export (Germain et al. 2010).

Corresponding author: H. Germain; E-mail: hugo.germain@uqtr.ca

*The *e*-Xtra logo stands for "electronic extra" and indicates that five supplementary figures and one supplementary table are published online.

The contribution of mRNA export to plant immunity was demonstrated in the study of *mos3* and *mos11* mutants (Germain et al. 2010; Zhang and Li 2005). MOS3/SAR3/AtNUP96 is an integral nucleopore component of the conserved Nup107-160 complex and is required for mRNA export (Parry et al. 2006). MOS11 is a conserved nuclear protein with homology to human RNA-binding protein CIP29 (cytokine-induced protein 29kDa), which does not associate with the nuclear pore. We have shown that *mos11* plants display increased nuclear accumulation of mRNAs compared with wild type (WT) (Germain et al. 2010), thereby linking MOS11 to mRNA export. Consistent with this, the mammalian MOS11 ortholog CIP29 was found to interact with ALY, a protein involved in mRNA export via UAP56 (U2AF65-associated protein 56), an RNA helicase with 91% identity to DDX39 (DEAD [Asp-Glu-Ala-Asp] box polypeptide 39B) (Dufu et al. 2010; Meissner et al. 2003). Biochemical analysis performed in human and *Drosophila* spp. further illustrated that CIP29 interacts with FUS/TLS (fused in sarcoma/translocated in sarcoma) and the RNA helicase DDX39 (Dufu et al. 2010; Leaw et al. 2004; Sugiura et al. 2007) to enhance its helicase activity (Sugiura et al. 2007).

Here, we report a systematic reverse genetic analysis of the knockout lines of the closest *Arabidopsis* homologs corresponding to the human/*Drosophila* mRNA export complex composed of hDDX39/hUAP56, hFUS/TLS, and hALY. Our findings demonstrate that one member of the complex, TAF15b (homolog of FUS/TLS), can partially suppress the defense-associated phenotypes of *snc1*. In addition, in triple mutant *mos11-1 taf15b snc1* plants, the morphological and autoimmune phenotypes associated with *snc1* are almost completely abrogated. We also observed that TAF15b localizes to RNA processing bodies (p-bodies), structures involved in mRNA decay, including nonsense-mediated mRNA decay (NMD), AU-rich element-mediated mRNA decay, and micro (mi)RNA-induced mRNA silencing (Kulkarni et al. 2010). TAF15b seems to contribute to SNC1 homeostasis at posttranscriptional levels. Recent findings showed that mutants impaired in NMD have constitutive defense responses (Gloggnitzer et al. 2014) and that PAT1 (a decapping enhancer) is part of the MPK4-mediated defense signaling pathway in response to flagellin (Roux et al. 2015), provide additional evidence that mRNA decay is linked to the regulation of plant immunity.

RESULTS

taf15b partially suppresses the autoimmune phenotypes of *snc1*.

In human and *Drosophila* spp., the CIP29 protein interacts with three partners, namely, DDX39, FUS/TLS, and ALY. DDX39 is an RNA helicase highly similar to UAP56, a RNA helicase well-known for its involvement in mRNA export (Carmody and Wente 2009; Chi et al. 2012; Dufu et al. 2010; Katahira 2012). FUS/TLS is a family of RNA-binding proteins that includes TATA-box binding factors (TAFs). Beyond their RNA binding capacity, TAFs influence the initiation of transcription (Dikstein et al. 1996; Mizzen et al. 1996; Pham and Sauer 2000). ALY is a nuclear protein with nucleic acid–binding ability. ALY has been shown to interfere with silencing in plants (Canto et al. 2006; Uhrig et al. 2004). Through BLAST analysis, we identified the closest homologs of DDX39, FUS/TLS, and ALY in *Arabidopsis* (Table 1). We then obtained homozygous T-DNA knockout lines for each gene and crossed them with *snc1* plants, to monitor if mutations in these members of the CIP29 complex could affect *snc1* signaling similarly as *mos11*.

The stunted morphology of *snc1* was partly suppressed in the *taf15b snc1* double mutant plants (Fig. 1A). However, none of the other double mutants with *snc1* resulted in *snc1* suppression (not shown). In addition to their stunted morphology, *snc1* plants display increased resistance to virulent oomycete pathogen *H. arabidopsidis* Noco2 (Li et al. 2001). To assess if *taf15b* could also suppress this *snc1* phenotype, we performed an infection assay with *H. arabidopsidis* Noco2. The *taf15b snc1* plants did not display a statistically significant difference from *snc1* plants (Fig. 1B). Similarly to *mos11-1*, the single *taf15b* plant did not display enhanced disease susceptibility when compared with WT plants. In contrast to *mos11-1* plants, *taf15b* plants did not display impaired mRNA export (Supplementary Fig. S1). We also assessed the capacity of *taf15b* to alter the constitutive resistance of *snc1* to virulent bacterial pathogen *P. syringae* pv. *maculicola* ES4326. In this case, the suppression of the *snc1* resistance was significant (Fig. 1C). Since *snc1* immune activation can be monitored by the level of expression of *PR* genes (Li et al. 2001), we verified if the *PR* gene expresssion level was affected in *taf15b snc1* plants. The quantitative reverse transcription-polymerase chain reaction (RT-PCR) data demonstrates that *snc1* plants express *PR1* transcript at a level approximately 500 times (486-fold) higher than observed in unstressed WT plants (Fig. 1D). In the double mutant *taf15b snc1* plants, *PR1* expression level was approximately half the level observed in *snc1*, at 233-fold of the WT plants. For *PR2* expression, similar fold changes were observed (Fig. 1D).

In conclusion, among all CIP29 complex component mutants tested, *taf15b* is the only mutant that affects the *snc1* autoimmune phenotypes, acting as a partial suppressor of *snc1*.

TAF15 and TAF15b have different topology and are functionally distinct.

Since *Arabidopsis* contains another FUS/TLS homolog, TAF15, we investigated whether it was redundant to TAF15b. In order to assess whether TAF15 and TAF15b were functionally redundant, we compared the morphology of *taf15* and *taf15b* T-DNA knock-out lines to that of the *taf15 taf15b* double mutant. The *taf15* plants are indistinguishable from WT, whereas the *taf15b* mutant is slightly different from WT, with slightly bigger and rounder leaves, often concave rather than convex, indicating that, in *Arabidopsis*, the TAF15 protein cannot functionally complement *taf15b* morphological phenotypes (Fig. 2A). The *taf15 taf15b* double mutant resembles the *taf15b* single mutant (Fig. 2A). To further substantiate the difference between *taf15b* and WT plants and

Table 1. CIP29 direct and indirect interactors and their putative *Arabidopsis* homolog

Human gene	Gene function	Homolog in *Arabidopsis*	Available T-DNA/location
DDX39	DEAD box RNA helicase	At5g11170	SALK_101221/intron
FUS/TLS TAF15b	Spliceosome assembly and transcriptional control	At5g58470	SALK_061974/intron SAIL_35_B06/intron
ALY (indirect)	Splicing factor linking premRNA splicing to mRNA export	At5g02530	SALK_094909/5′ untranslated region WiscDsLox461-464N10/exon
		At5g59950	SAIL_381_E08/exon WiscDsLox493E08/promoter

between *taf15b* and *taf15*, we evaluated the number of rosette leaves when the plants were 5 weeks old, as the *taf15b* mutant exhibits a late-flowering phenotype. As shown in Figure 1B, *taf15b* and *taf15b taf15* double mutant plants exhibit similar flowering-time defects, confirming that these two genes do not have redundant functions. Furthermore, the phylogenetic tree generated using the full-length amino acid sequences of AtTAF15 and AtTAF15b homologs found in different plant species also shows that AtTAF15 and AtTAF15b form different clades in all species (Fig. 2C).

While TAF15 and TAF15b have similarity in composition of their functional domains, their protein architecture is different. TAF15 possesses a RNA-recognition motif at its amino terminus, followed by a two–zinc finger domain, whereas in TAF15b only one zinc finger is present (Fig. 2D). The human TAF15 protein has the protein topology of AtTAF15, while FUS/TLS shares the protein topology of AtTAF15b. For further analysis, we therefore refer to AtTAF15b as the homolog of FUS/TLS rather than that of human AtTAF15.

With publicly available microarray data (Winter et al. 2007), we asked whether *TAF15*, *TAF15b*, *MOS11*, and *SNC1* gene expression was inducible by virulent bacterial pathogen *Pseudomonas syringae* DC3000, avirulent oomycete pathogen *H. arabidopsidis* Emwa1, virulent oomycete pathogen *H. arabidopsidis* Noco2, and PAMP elicitor flg22. The expression of these genes was not significantly modulated in the assessed conditions (Supplementary Fig. S2).

In order to assess if *taf15b*, *taf15*, or the *taf15 taf15b* mutations would impair the immune capacity of other NLR proteins, we evaluated the response of these mutants against the avirulent bacterial pathogen *Pseudomonas syringae* pv. *tomato* DC3000 *AvrRpt2* (Supplementary Fig. 3A), *P. syringae* pv. *tomato* DC3000 *AvrRPS4*, and the avirulent oomycete strain *H. arabidopsidis* Emwa1. We also evaluated PTI, using the type III secretion–deficient bacterial strain *P. syringae* pv. *tomato* DC3000 *hrcC*–. Response to the avirulent pathogens tested or *P. syringae* pv. *tomato* DC3000 *hrcC*– was not affected in either single mutants or the double mutant, indicating that neither TAF15b nor TAF15 is a component involved in general NLR signaling. We also assessed the reactive oxygen species (ROS) induction capacity in WT, *taf15*, *taf15b*, and *taf15 taf15b* plants (Supplementary Fig. S4) in response to flg22. Interestingly, we observed mild yet reproducible reduction in ROS induction by flg22 in the *taf15b* single mutant and the *taf15 taf15b* double mutant. Based on the phylogeny and protein topology, we conclude that the closest homolog of AtTAF15b in humans is FUS/TLS. In addition, based on our epistatic analysis (discussed below), we conclude that AtTAF15 and AtTAF15b do not have overlapping functions in plants. Finally, neither TAF15 nor TAF15b appears to be involved in general NLR signaling. However, they do contribute to the ROS induction in PTI.

mos11-1 taf15b snc1 triple mutant analysis.

Since *taf15b*, like *mos11-1*, could partially suppress the *snc1* phenotype, we sought to investigate if the lack of these two proteins would have an additive effect on the suppression of the *snc1* autoimmune phenotypes. While both double mutants were only partial *snc1* suppressors, the triple mutant *mos11-1 taf15b snc1* almost fully suppressed the stunted morphology of *snc1* (Fig. 3A). However, the triple mutant plants had delayed bolting when compared with WT plants (Fig. 3A). Since *snc1* dwarf morphology was fully suppressed in the triple mutant, we verified whether *PR* gene expression was comparable to levels observed in WT. Indeed, we observed that the *PR* gene expression in the triple mutant was very close to that observed in WT plants (Fig. 3B).

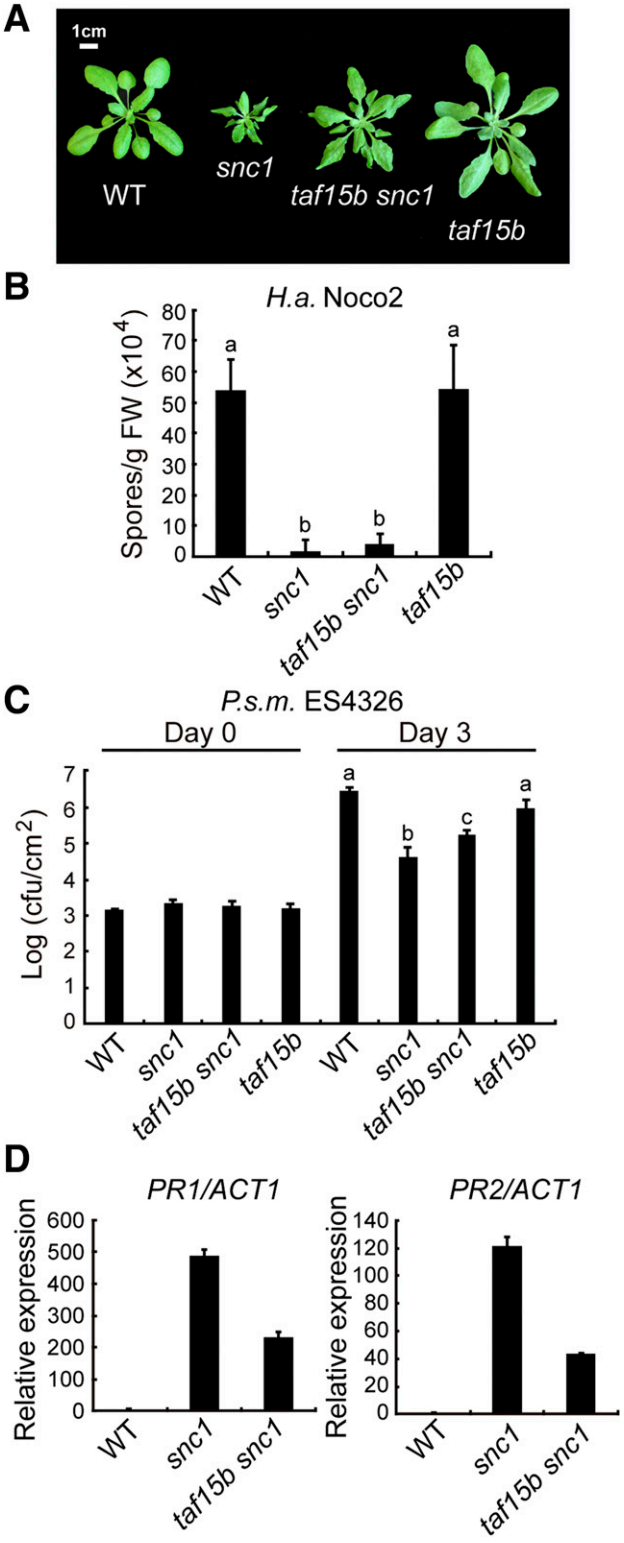

Fig. 1. *taf15b* partially suppresses the autoimmunity of *snc1*. **A,** Morphology of 4-week-old soil-grown wild type (WT), *snc1*, *taf15b snc1*, and *taf15b* plants. **B,** Two-week-old soil-grown plants were inoculated with *Hyaloperonospora arabidopsidis* Noco2 at a concentration of 50,000 conidiospores per milliliter and the number of conidiospores was quantified 7 days after inoculation. Bars represent the mean of four replicates. Statistical significance was established using Student *t* test ($P < 0.05$) and statistically different results are represented by different letters. **C,** Five-week-old soil-grown plants were inoculated with *Pseudomonas syringae* pv. *maculicola* ES4326 at an optical density at 600 nm = 0.0001, and statistical significance was evaluated using Student's *t* test ($P < 0.05$) **D,** *PR1* and *PR2* gene expression was quantified using quantitative reverse transcription-polymerase chain reaction and was normalized with *ACT1*.

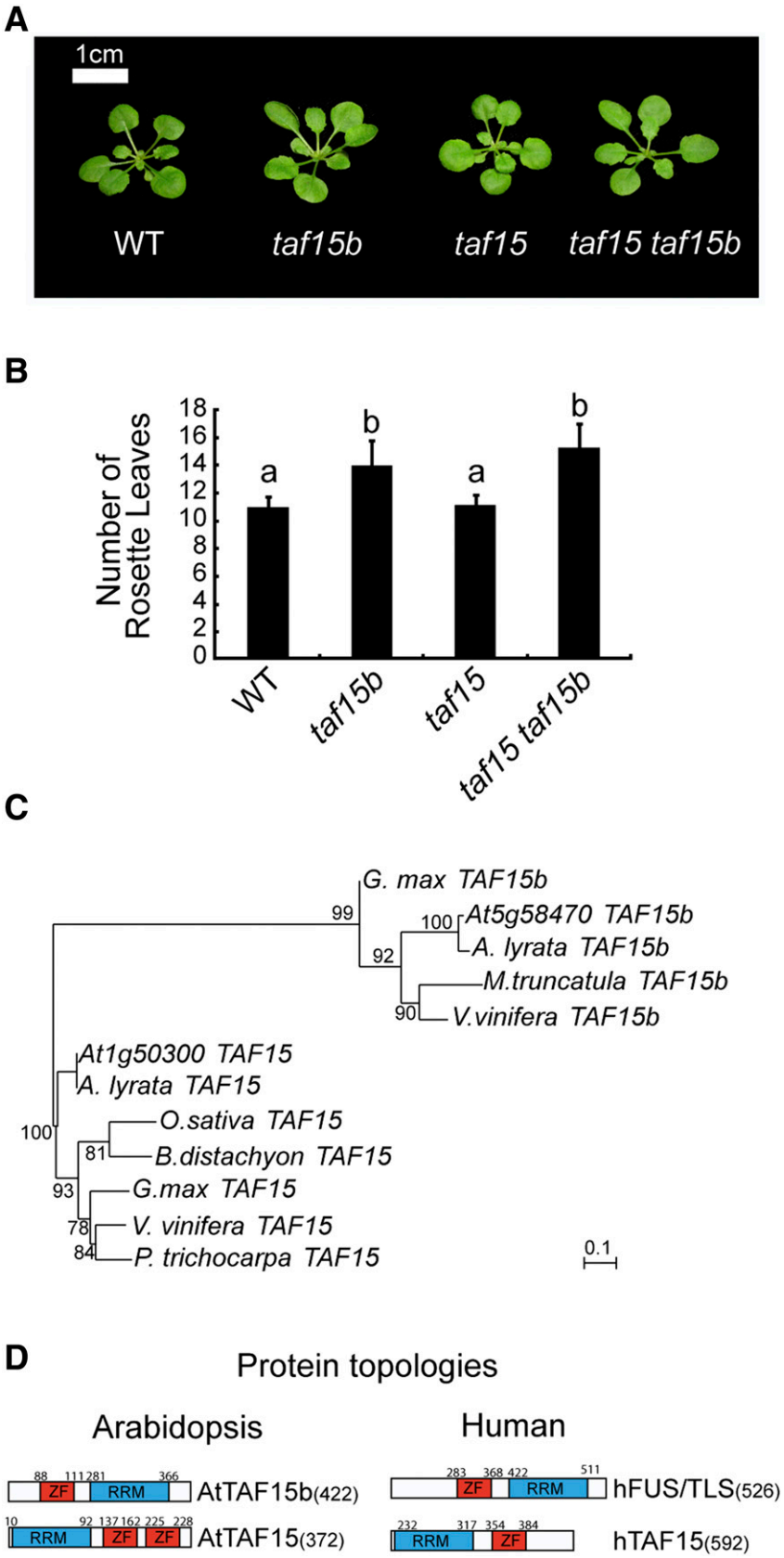

Fig. 2. TAF15 and TAF15b have different topology and are functionally distinct. **A,** Morphology of 2.5-week-old soil-grown wild type (WT), *taf15b*, *taf15*, and *taf15 taf15b* plants. **B,** Comparing flowering time in soil-grown WT, *taf15b*, *taf15*, and *taf15 taf15b*. Letters indicate statistical significance as determined by Student's *t* test ($P < 0.0001$). **C,** Phylogeny of TAF15b-related proteins was inferred, using the full-length amino acid sequences. Alignment and tree was computed using ClustalW and a neighbor-joining alignment was used. **D,** Protein domain organization was inferred using the National Center for Biotechnology Information conserved domain database software. Small numbers above the proteins indicate the relative position of the domains; the numbers at the end of the protein names indicate the number of amino acids.

Since the morphology suppression and *PR* gene expression suppression of the autoimmune mutant was nearly complete, we assessed the resistance of the triple mutant plants to the virulent biotrophic oomycete *H. arabidopsidis* Noco2. The triple mutant analysis showed an additive effect of the *mos11* and the *taf15b* mutations in the suppression of *snc1* resistance to *H. arabidopsidis* Noco2 (Fig. 3C). The additive effect of the *taf15b* mutant on the *snc1 mos11* mutant, both at the morphological level, in the resistance to pathogens and the absence of mRNA export defect in *taf15b* suggests that MOS11 and TAF15b proteins do not have a role in the same pathway.

TAF15b does not associate with MOS11 in planta.

To further assess whether Taf15b could associate with MOS11 in planta as CIP29 does with FUS (Dufu et al. 2010), we generated a stable epitope-tagged transgenic line expressing *TAF15b-FLAG* under the control of its own regulatory sequence (1,436 bp upstream of the start codon) in *taf15b* background. This construct fully complements the *taf15b snc1* phenotype (Fig. 4A), suggesting that the C-terminal FLAG tag does not affect the function of TAF15b. We then crossed this line with *MOS11-green fluorescent protein* (*GFP*) (in *mos11-1* background) to generate F1 plants heterozygous at both loci that could be used for coimmunoprecipitation. In MOS11-GFP, we could not immunoprecipitate TAF15b-FLAG (Fig. 4B). This result, combined with the additive effect of *mos11* and *taf15b* in the triple mutant, suggest that MOS11 and TAF15b either do not physically interact in plants and are not involved in the same biological function or their interaction is too weak or transient to be detectable. Additionally, we queried the Plant Interactome database (*Arabidopsis* Interactome Mapping Consortium 2011) to search for other proteins that could interact with TAF15b. This database reported that TAF12b (Kubo et al. 2011), TAF4b, TAF14 (Choi et al. 2011), TAF5, and TAF4 all interact with TAF15b (Supplementary Table S1) but not with MOS11 or TAF15.

Subcellular localization of TAF15b.

TAF15b encodes a glycine-rich protein of 42 kDa. It contains a zinc-finger domain (position 87 to 111), a RNA recognition motif (position 281 to 360) (predicted by PFAM) and is predicted to be nuclear localized by the WoLF PSORT prediction tool. Since TAF15 proteins have not been well characterized in plants, we further investigated the subcellular localization of TAF15b. When *TAF15b-GFP* under the control of its native promoter was transformed in the *taf15b snc1* double mutant, the transformed plants displayed *snc1*-like morphology, indicating that TAF15b was properly expressed and the fusion gene is able to complement the *taf15b* defects (Fig. 5A). Although TAF15b-GFP could be observed in the nuclei (Fig. 5B), strong fluorescence was also observed as clear punctate spots in the cytosol (Fig. 5C and E), reminiscent of proteins localized to p-bodies. To assess if these could be p-bodies, we used a stable *Arabidopsis* transgenic line expressing the cyan fluorescent protein (CFP)–labeled p-bodies marker DECAPPING 1 (Xu et al. 2006) (pDCP1:DCP1-CFP). Similar punctate spots as observed in *TAF15b-GFP* plants were observed (Fig. 5F, H, and J). To further confirm that Taf15b-GFP was indeed localized to p-bodies, we crossed the *TAF15b-GFP* line with the *DCP1-CFP* line and examined F1 plants. A clear CFP and GFP colocalization was observed (Fig. 5K and L; Supplementary Fig. S5), indicating that TAF15b localizes to the p-bodies.

***taf15b* affects SNC1 protein accumulation.**

P-bodies are known to be involved in the sequestration of mRNAs, NMD, AU-rich element–mediated mRNA decay, and microRNA induced mRNA silencing (Kulkarni et al. 2010). All

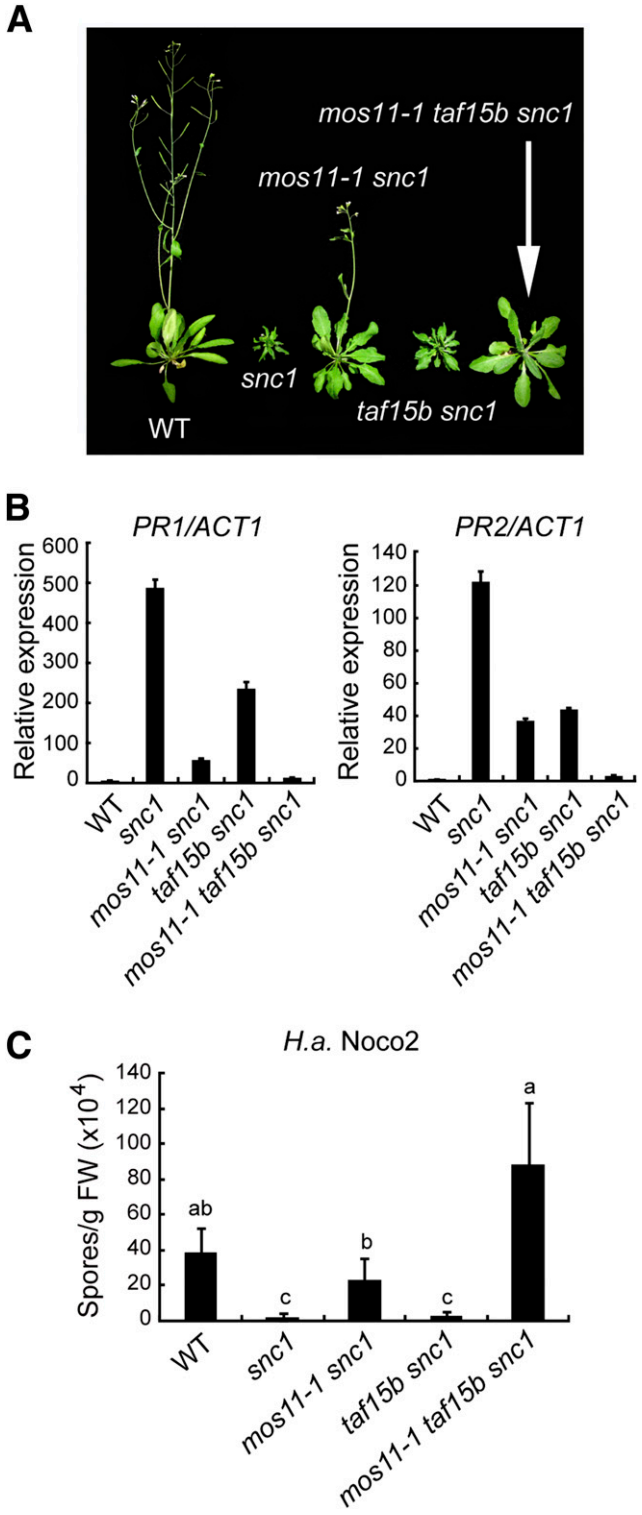

Fig. 3. *mos11-1 taf15b snc1* triple mutant analysis. **A,** Morphology of wild type (WT), *snc1*, *mos11 snc1*, *taf15b snc1*, and *mos11 taf15b snc1* plants. Soil-grown plants were photographed 5 weeks after germination. **B,** Expression of defense marker genes *PR1* and *PR2* in the indicated genotypes. Quantitative reverse transcription-polymerase chain reaction was performed on 2-week-old plants grown on ½ Murashige Skoog plates. *ACT1* was used to normalize the transcript levels. Each average represents three technical repeats. **C,** Growth of *Hyaloperonospora arabidopsidis* Noco2 7 days after inoculation on the indicated genotypes. Spray-infection was performed on 2-week-old plants on soil with a conidiospore suspension at 100,000 spores per milliliter. Each average represents four sampling repeats. Letters indicate statistical significance as determined by Student's *t* test ($P < 0.02$). The experiment was repeated three times with similar results.

these components of RNA regulation and catabolism may affect transcription and translation of specific mRNAs. In addition, plant NLR proteins are known to be regulated by transacting small interfering RNAs (Zhai et al. 2011). Thus, we examined whether the level of *SNC1* transcript or the level of SNC1 protein was affected in *taf15b* and *taf15b snc1*, relative to WT and *snc1* plants. We did not observe significant differences in mRNA levels between WT and *taf15b* and between *snc1* and *snc1 taf15b* (Student's *t*-test, in both cases $P > 0.1$) (Fig. 6A). We then tested whether SNC1 protein accumulation is affected by *taf15b*, through Western blot assay using an anti-SNC1 antibody (L-i et al. 2010). We consistently observed decreased SNC1 protein level in *taf15b* compared with WT, and this difference in maintained in *snc1 taf15b* compared with *snc1* (Fig. 6B and C). As the *SNC1* transcription is not substantially affected by *taf15b* (Fig. 6A), we conclude that *taf15b* affects SNC1 protein accumulation through posttranscriptional mechanisms.

***taf15b* does not affect miRNA accumulation.**

Given the localization displayed by TAF15b and the apparent lack of a direct effect on *SNC1* mRNA level, the suppression of the *snc1* phenotype is likely indirect. Putative targets could be regulated by miRNA and affect TNL-mediated immunity. To test this hypothesis, we assessed the level of known miRNAs in our genetic backgrounds (Fig. 7). Northern blot analysis showed slight differences for some miRNA; however, when multiple repeats were performed, those differences were not found to be statistically significant. Therefore, we conclude that the effect of *taf15b* on *snc1* immunity is not via an obvious alteration of miRNA levels.

DISCUSSION

We have previously observed that *mos11*, through its defect in mRNA export, can partially suppress the phenotypes associated with the autoimmune mutant *snc1*. The human ortholog of MOS11, CIP29, associates with proteins involved in mRNA export: DDX39, ALY and FUS/TLS (TAF15b). Although the *Arabidopsis* genome has been analyzed for the presence of TAFs (Lago et al. 2004), very little is known about TAFs in plants. Here, we have performed a systematic reverse genetics analysis of the knockout lines corresponding to the closest *Arabidopsis* homologs of this complex and found that mutating *TAF15b* can partially suppress *snc1* autoimmunity.

TAFs or TATA-box binding protein–associated factors are main components in the assembly of the general transcription factor IID, required for the initiation of transcription by RNA polymerase II. Therefore, this *sensu stricto* definition would mean that TAF15b would have a role in transcription initiation, which is reinforced by the presence of a RNA-binding domain in the protein (Fig. 2) and a nuclear localization signal (Fig. 5). However, it is not known whether TAF15 proteins participate in the assembly of TFIID in plants. Here, we provide the first functional in planta analysis of *TAF15b*. We show evidence that TAF15b is involved in TNL-triggered immunity. Additionally, we observed that mutation of *TAF15b* enhances the *snc1*-suppressing effect of *mos11*, suggesting that they are not in the same pathway. Furthermore, TAF15b localizes to p-bodies, thereby strengthening the existing link between p-bodies and plant immune responses. SNC1 protein level is reduced in *taf15b* background, suggesting a role of TAF15b in regulating SNC1 accumulation, possibly posttranscriptionally. Its effect on SNC1 homeostasis explains the *snc1*-suppressing phenotypes of *taf15b*.

mRNA metabolism is a highly regulated and complex process. Following synthesis, mRNA molecules are processed in the nucleus, while concomitantly being loaded with proteins that will direct the messenger ribonucleoparticle (mRNP) toward the nucleopore. Upon traveling through the pore, mRNPs are accessible for translation in the cytosol. Stress-related translational slowdown may cause mRNAs to accumulate in stress granules. Alternatively, transcripts may also be stored in p-bodies to be made available later or targeted for degradation, thus providing an additional level of posttranscriptional control (Anderson and Kedersha 2006, 2009). Observed as cytoplasmic foci, p-bodies are the site of mRNA m^7GDP removal, the cap structure present at the 5′ end of all eukaryotic mRNAs. DCP2 (DECAPPING PROTEIN2) in association with DCP1 and VCS (VARICOSE) are sufficient for mRNA decapping (Xu et al. 2006), whereas DCP5 is also required for in vivo activity (Xu and Chua 2009). In mammalian cells, the RNA interference component Argonaute was shown to localize to p-bodies and interacts with GW182. Silencing of GW182 impairs silencing of microRNA reporters (Liu et al. 2005). P-bodies can have an opposite effect on viral replication. It was reported that p-body depletion enhances HIV production (Nathans et al. 2009), while some components of p-bodies represses replication of the *West Nile virus* and *Brome mosaic virus* (Beckham et al. 2007; Chahar et al. 2013). In plants, recovery from virus infection leads to translational repression of viral transcripts and a concomitant increase in p-body numbers and a *dcp2* mutant shows increased virus RNA accumulation and virus-induced gene silencing (Ma et al. 2015). In eukaryotes, the protein PAT1 (protein associated with topoisomerase II) acts as a decapping enhancer and localizes to the p-bodies (Ozgur et al. 2010). It was recently demonstrated that *A. thaliana* PAT1 is a substrate for MPK4, which is activated following flagellin treatment (Roux et al. 2015). Interestingly, *pat1* plants display increased *PR* gene expression that can be suppressed in *pat1 summ2* plants. SUMM2 is a resistance protein thought to guard MPK4 and suppresses autoimmunity caused by loss of different components of the MPK4 cascade (Zhang et al. 2012). It has previously been reported that impairment of NMD can trigger a constitutive immune response in *Arabidopsis* (Riehs-Kearnan

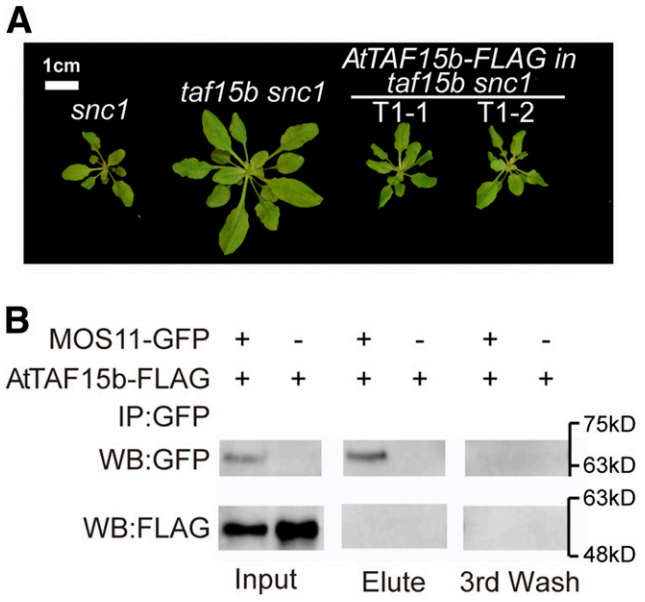

Fig. 4. TAF15b does not associate with MOS11 in vivo. **A,** Morphology of *snc1*, *taf15b snc1*, and two *taf15b snc1* transgenic lines expressing *AtTAF15b-FLAG* transgene. Soil-grown plants were photographed 4 weeks after germination. **B,** Immunoprecipitation of AtTAF15b-FLAG using anti–green fluorescent protein (GFP) antibody. Total protein extracts from seedlings grown on ½ Murashige Skoog plates were subjected to immunoprecipitation by anti-GFP agarose beads. Input and eluted samples were detected by anti-FLAG and anti-GFP antibodies.

et al. 2012). More recently, Gloggnitzer et al. (2014) showed that NMD contributed to the activation of a defense response through mRNA turnover alteration of a TNL immune receptor (Gloggnitzer et al. 2014). Together, these results point to the crucial roles RNA quality control and catabolism play in plant defense homeostasis.

TAFs are not accessory proteins whose sole role is the assembly of the general transcription factor TFIID. For example,

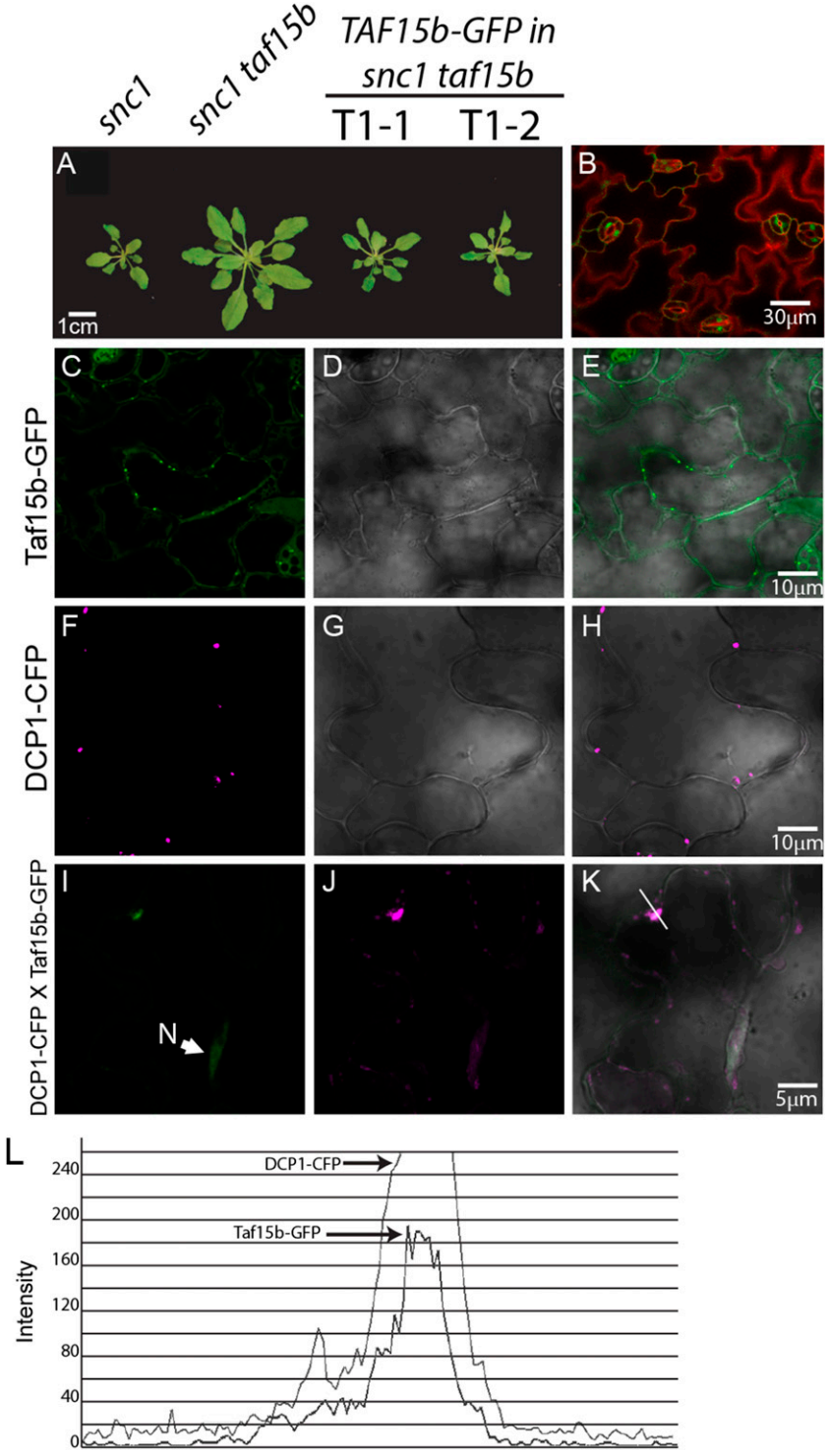

Fig. 5. Subcellular localization of TAF15b-GFP. **A,** Morphology of *snc1*, *taf15b snc1* and two *taf15b snc1* transgenic lines expressing *TAF15b-GFP* transgene. Soil-grown plants were photographed four weeks after germination. **B,** Green fluorescent protein (GFP) fluorescence in TAF15b-GFP transgenic plants. Leaf tissues of 5-day-old seedlings were stained with propidium iodide before imaging. **C,** TAF15b-GFP fluorescence in leaf epidermal cells of *taf15b* complemented with *TAF15b-GFP*. **D,** Differential interference contrast (DIC) image of the same region as in C. **E,** Overlay of the images in C and D. **F,** DCP1-cyan fluorescent protein (CFP) fluorescence in leaf epidermal cells of DCP-CFP plants. **G,** DIC image of the same region shown F. **H,** Overlay of images in F and G. **I,** TAF15b-GFP fluorescence in leaf epidermal cells of *TAF15b-GFP* × *DCP1-CFP* F1 plants. N indicates the nucleus. **J,** DCP1-CFP fluorescence in *TAF15b-GFP* × *DCP1-CFP* F1 plants. **K,** Overlap of images in I and J. **L,** Intensity plot of GFP (TAF15b-GFP) and DCP1 (CFP) in the p-bodies transected by the solid white line in panel K.

the well-characterized protein TAF1 has kinase, acetyltransferase, and ubiquitin-activating or conjugating enzyme activities. As such, it actively regulates transcription by chromatin decondensation and directly phosphorylates transcription factors (Dikstein et al. 1996; Mizzen et al. 1996; Pham and Sauer 2000). However, not all TAFs have been well characterized. In mammalian cells, TAF15 is a member of the highly conserved TET protein family of RNA binding proteins (also known as FET), which comprises FUS and Ewing sarcoma protein. TET proteins are involved in several diseases, including the onset of specific tumors. Human TAF15 was shown to associate with RNA polymerase II (Bertolotti et al. 1996), a more recent report has shown that TAF15 interacts with the U1 snRNP spliceosomal subunit (Leichter et al. 2011). When Marko et al. (2012) examined the subcellular localization of TAF15, they observed that, while a nuclear localization is the prevalent location of TAF15 in some cell types, the carboxy-terminal RGG repeat motif directs TAF15 to cytosolic granules. Interestingly, *Arabidopsis* TAF15b possesses an RGG-rich region in its C-terminus (amino acids 381 to 402 RGGGRGGGGGGYGGGGG) as well. As Marko et al. (2012) observed, colocalization of the p-body marker DCP1 and TAF15 and also, importantly, FUS localize to RNA granules in mammals (Han et al. 2012); these results are in direct agreement with our results (Fig. 5), in which we observed AtTAF15b colocalizing with DCP1 in p-bodies. However, the precise role of *Arabidopsis* TAF15b in p-bodies remains unknown. Our results show that TAF15b does not affect the accumulation of *SNC1* mRNA or small RNA; however, it does affect SNC1 protein accumulation. As other TNL-mediated immunity is not affected in *taf15b* plants, we speculate that TAF15b likely specifically affects SNC1-mediated immunity through regulating the stability of its mRNA or its posttranscriptional RNA processing steps in the p-bodies.

Our results indicate that MOS11 and TAF15b act in different pathways, MOS11 regulates mRNA export while the exact role of TAF15b remains to be elucidated. As TAF15b localizes both to the nucleus and p-bodies, we speculate that it is a multifunctional protein. Although we originally hypothesized that it

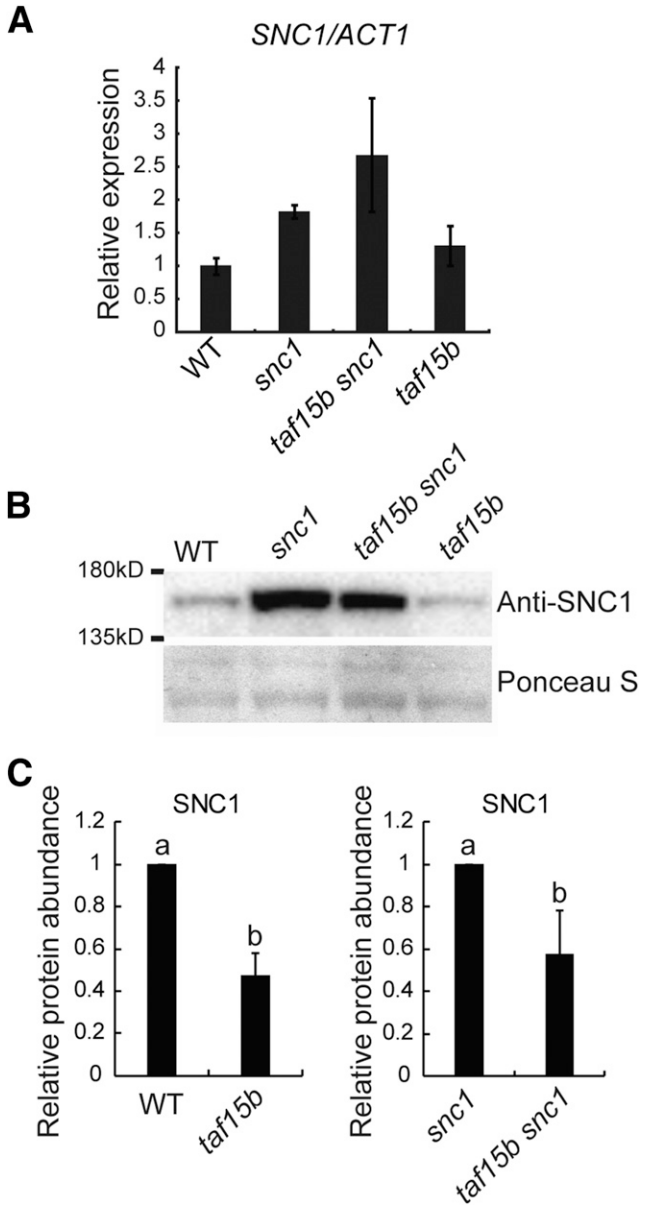

Fig. 6. *taf15b* does not affect *SNC1* transcript but does reduce SNC1 protein level. **A,** Quantitative reverse transcription-polymerase chain reaction was used to quantify the *SNC1* transcript levels in various genotypes. **B,** Western blot using anti-SNC1 antibody to quantify the SNC1 protein levels in wild type (WT), *snc1*, *taf15b snc1*, and *taf15b*. The experiment was repeated four times. The same plants were used for experiments in A and B. Leaf tissue was collected from 4-week-old soil-grown plants. **C,** Quantification of SNC1 band intensity relative to a nonspecific band in Ponceau S in four Western blot repeats as described in B, as determined by using Image J. Bars represent mean ± standard deviation of relative SNC1 protein abundance. SNC1 protein abundance in WT (left panel) or *snc1* (right panel) was set as 1. Student's *t* tests were used to calculate the statistical significance between genotypes, as indicated by different letters ($P < 0.05$).

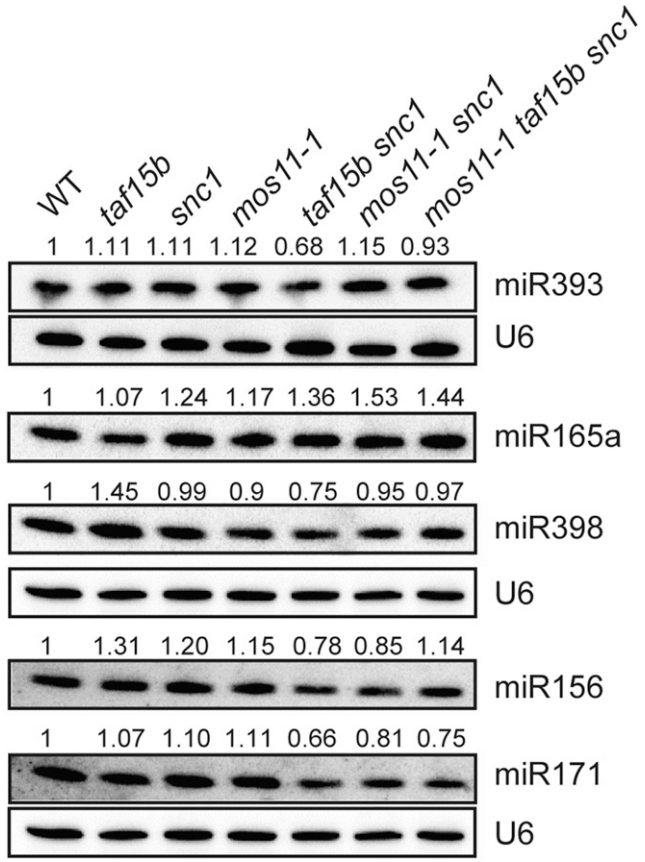

Fig. 7. *taf15b* does alter the level of some micro (mi)RNAs. The expression level of five miRNAs (miR393, miR165a, miR393, miR398, miR156, and miR171) was assessed and quantified by Northern blot for plant genotypes WT (wild type), *taf15b*, *snc1*, *mos11-1*, *taf15b snc1*, *mos11-1 snc1*, and *mos11 taf15b snc1*. Loading control was normalized by U6 RNA. RNA was extracted from the leaves of 4-week-old plants.

may contribute to mRNA export, our data did not support a mRNA export defect in *taf15b*. We cannot exclude the possibility that it still serves a role in mRNA export, but the defect in the mutant is too weak to be detected with the assay we are using. Based on our data, we cannot exclude the possibility that MOS11 and TAF15b still function in a complex in the nucleus for mRNA export in which the two proteins do not interact directly with each other. However, the cytosolic p-body localization of TAF15b suggests its independent function, which is supported by our genetic analysis; whether animal TAF15b behaves similarly in the cytosol remains to be determined. Its localization in the p-bodies indicates its involvement in, perhaps, RNA turnover and mRNA homeostasis control. However, the limited targets we examined, including *SNC1* and some selected miRNAs, did not reveal general striking RNA level defects, only an apparent effect on SNC1 protein accumulation. According to its weak phenotypes, we believe that possible defects in RNAs may also be too small to be detected using the current methods. Further analysis is needed to decipher the exact biochemical role of TAF15b.

MATERIALS AND METHODS

Protein topologies and phylogenetic tree.

Protein topology was searched using the National Center for Biotechnology Information Conserved Domain search tool. The phylogenetic tree was made using Colbalt Protein Alignment software, set to infer the tree using a neighbor-joining method from the full-length amino acid sequences. The species and protein models used to infer the tree are for TAF15b proteins *Arabidopsis thaliana* At5g58470, *Glycine max* XP_003518322, *Arabidopsis lyrata* XP_002866269, *Medicago truncatula* XP_003599332, *Vitis vinifera* XP_002269146, and for TAF, *Arabidopsis thaliana* At1g50300, *Arabidopsis lyrata* XP_002894246, *Oryza sativa* BAD33184, *Brachypodium distachyon* XP_003562545, *Glycine max* NP_001241952, *Vitis vinifera* XP_002273586, and *Populus trichocarpa* XP_002315063. The human protein FUS/TLS and TAF15 used to infer the topologies were AAC35285 and Q92804, respectively.

Plant growth, construction of plasmids, and plant transformation.

Plants were grown at 22°C under 16-h-light and 8-h-dark regime. To create *AtTAF15b-GFP* and *AtTAF15b-FLAG* constructs, a genomic PCR fragment of *AtTAF15b* (At5g58470) with 1,436 bp upstream from the start codon was cloned into the modified binary vector pCam1305 with either C-terminal GFP or FLAG sequence by restriction enzymes *Bam*HI and *Sal*I. The cloning PCR was performed using primers 5′-CGC GGATCCCATTTCTCCAGAGCTATGGC-3′ and 5′-ACGCA CGCGTCGACATATGGACGAGACCGGTTTC-3′. *Agrobacterium*-mediated plant transformation was carried out with slight modification to the procedure described by Clough and Bent (1998). Briefly, the Silwet L-77 was substituted with OFX-309 and floral dip was performed twice with a 1-week interval between dippings (Mireault et al. 2014).

Screen for homozygous T-DNA mutants.

To identify homozygous *taf15b* T-DNA Salk_061974 or Sail_35_B06 mutants, we used primers 5′-CAAAACAATCC ACCACCATTC-3′ and 5′-AAAAAGTCAAGCAGTGCGATG-3′ to perform PCR. Similarly, to check homozygosity for the *mos11-1* mutation, primers 5′-CGGCCGATAATTCGTGGACG-3′ and 5′-CACCAGTAGATAGCCCTCC-3′ were used. For presence of the T-DNA from the generic primers, LBb1.3 (ATTTTG CCGATTTCGGAAC) was used for SALK lines and Sail-F (cgtccgcaatgtgttattaag) for SAIL lines.

RT-PCR analysis and pathogen infections.

RT-PCR analysis of the expression of *PR1* and *PR2* was carried out as previously described (Cheng et al. 2011). *ACT1* was used as loading control. Leaf infiltration of *Pseudomonas syringae* strains was performed on 4-week-old plants as described previously (Li et al. 1999). Spray infection by *H. arabidopsidis* Noco2 or Emwa1 was performed as described previously (Li et al. 1999).

Confocal microscopy and in situ total mRNA hybridization.

Ten-day-old plants grown on ½ Murashige-Skoog (MS) were used for observation with GFP- or CFP-tagged constructs, using a Leica SP8 confocal microscope. In situ poly-A RNA hybridization was performed as previously described (Germain et al. 2010).

Nuclear extraction, coimmunoprecipitation, and Western blot analysis.

F1 plants from a cross between plants homozygous for *MOS11-GFP* in *mos11-1* and *AtTAF15b-FLAG* in Salk_061974 were used to check the association between TAF15b and MOS11 in vivo, while plants homozygous for *AtTAF15b-FLAG* in Salk_061974 were used as the negative control. Plants were grown on MS medium and 5 g of 2.5-week-old plants were harvested from each genotype. Nuclear extraction was performed as previously described (Wiermer et al. 2012). Nuclei (in NE-3 buffer: 20 mM HEPES-KOH, pH 7.9, 2.5 mM $MgCl_2$, 150 mM NaCl, 20% glycerol, 0.2% Triton X-100, 0.2 mM EDTA, and 1 mM dithiothreitol, with protease inhibitors) were sonicated using a 550 Sonic Dismembrator (Fisher) at a power of 2.75 for 4 min with a 10-s pause for each 5 s of operation, to break the nuclear envelope. Nuclear samples were incubated with NHS-activated sepharose beads (GE Healthcare) for 30 min to remove nonspecific binding. Nuclei were pelleted at 5, 000 × *g* for 30 s and were allowed to be incubated with recombinant camel GFP-binding protein–conjugated beads for 3 h. After incubation, the beads were pelleted at 20,000 × *g* for 5 min and were washed three times with NE-3. Subsequent Western blot was performed using anti-GFP and anti-FLAG antibodies respectively (Roche).

ROS assay.

Eight leaf discs (4 × 4 mm) of 4-week-old *Arabidopsis* plants were sampled using a razor blade and were floated overnight under light on sterile water. PAMP-induced ROS produced by the leaf discs were measured by a luminol-based assay (Lu et al. 2010; Trujillo et al. 2008). Luminescence was captured using a Tecan M200 plate reader.

LITERATURE CITED

Anderson, P., and Kedersha, N. 2006. RNA granules. J. Cell Biol. 172: 803-808.

Anderson, P., and Kedersha, N. 2009. RNA granules: Post-transcriptional and epigenetic modulators of gene expression. Nat. Rev. Mol. Cell Biol. 10:430-436.

Arabidopsis Interactome Mapping Consortium. 2011. Evidence for network evolution in an *Arabidopsis* interactome map. Science 333:601-607.

Ausubel, F. M. 2005. Are innate immune signaling pathways in plants and animals conserved? Nat. Immunol. 6:973-979.

Beckham, C. J., Light, H. R., Nissan, T. A., Ahlquist, P., Parker, R., and Noueiry, A. 2007. Interactions between brome mosaic virus RNAs and cytoplasmic processing bodies. J. Virol. 81:9759-9768.

Bertolotti, A., Lutz, Y., Heard, D. J., Chambon, P., and Tora, L. 1996. hTAF(II)68, a novel RNA/ssDNA-binding protein with homology to the pro-oncoproteins TLS/FUS and EWS is associated with both TFIID and RNA polymerase II. EMBO (Eur. Mol. Biol. Organ.) J. 15: 5022-5031.

Boller, T., and Felix, G. 2009. A renaissance of elicitors: Perception of microbe-associated molecular patterns and danger signals by pattern-recognition receptors. Annu. Rev. Plant Biol. 60:379-406.
Bowling, S. A., Guo, A., Cao, H., Gordon, A. S., Klessig, D. F., and Dong, X. 1994. A mutation in Arabidopsis that leads to constitutive expression of systemic acquired resistance. Plant Cell 6:1845-1857.
Caillaud, M. C., Asai, S., Rallapalli, G., Piquerez, S., Fabro, G., and Jones, J. D. 2013. A downy mildew effector attenuates salicylic acid-triggered immunity in Arabidopsis by interacting with the host mediator complex. PLoS Biol. 11:e1001732.
Canto, T., Uhrig, J. F., Swanson, M., Wright, K. M., and MacFarlane, S. A. 2006. Translocation of *Tomato bushy stunt virus* P19 protein into the nucleus by ALY proteins compromises its silencing suppressor activity. J. Virol. 80:9064-9072.
Carmody, S. R., and Wente, S. R. 2009. mRNA nuclear export at a glance. J. Cell Sci. 122:1933-1937.
Chahar, H. S., Chen, S., and Manjunath, N. 2013. P-body components LSM1, GW182, DDX3, DDX6 and XRN1 are recruited to WNV replication sites and positively regulate viral replication. Virology 436: 1-7.
Cheng, Y. T., Germain, H., Wiermer, M., Bi, D., Xu, F., García, A. V., Wirthmueller, L., Després, C., Parker, J. E., Zhang, Y., and Li, X. 2009. Nuclear pore complex component MOS7/Nup88 is required for innate immunity and nuclear accumulation of defense regulators in *Arabidopsis*. Plant Cell 21:2503-2516.
Cheng, Y. T., Li, Y., Huang, S., Huang, Y., Dong, X., Zhang, Y., and Li, X. 2011. Stability of plant immune-receptor resistance proteins is controlled by SKP1-CULLIN1-F-box (SCF)-mediated protein degradation. Proc. Natl. Acad. Sci. U.S.A. 108:14694-14699.
Chi, B., Wang, Q., Wu, G., Tan, M., Wang, L., Shi, M., Chang, X., and Cheng, H. 2012. Aly and THO are required for assembly of the human TREX complex and association of TREX components with the spliced mRNA. Nucleic Acids Res. 41:1294-1306
Chisholm, S. T., Coaker, G., Day, B., and Staskawicz, B. J. 2006. Host-microbe interactions: Shaping the evolution of the plant immune response. Cell 124:803-814.
Choi, K., Kim, J., Hwang, H. J., Kim, S., Park, C., Kim, S. Y., and Lee, I. 2011. The FRIGIDA complex activates transcription of *FLC*, a strong flowering repressor in *Arabidopsis*, by recruiting chromatin modification factors. Plant Cell 23:289-303.
Clarke, J. D., Liu, Y., Klessig, D. F., and Dong, X. 1998. Uncoupling PR gene expression from NPR1 and bacterial resistance: Characterization of the dominant Arabidopsis *cpr6-1* mutant. Plant Cell 10: 557-569.
Clough, S. J., and Bent, A. F. 1998. Floral dip: A simplified method for *Agrobacterium*-mediated transformation of *Arabidopsis thaliana*. Plant J. 16:735-743.
Collier, S. M., and Moffett, P. 2009. NB-LRRs work a "bait and switch" on pathogens. Trends Plant Sci. 14:521-529.
Dikstein, R., Ruppert, S., and Tjian, R. 1996. $TAF_{II}250$ is a bipartite protein kinase that phosphorylates the base transcription factor RAP74. Cell 84: 781-790.
Dufu, K., Livingstone, M. J., Seebacher, J., Gygi, S. P., Wilson, S. A., and Reed, R. 2010. ATP is required for interactions between UAP56 and two conserved mRNA export proteins, Aly and CIP29, to assemble the TREX complex. Genes Dev. 24:2043-2053.
Fontes, E. P., Santos, A. A., Luz, D. F., Waclawovsky, A. J., and Chory, J. 2004. The geminivirus nuclear shuttle protein is a virulence factor that suppresses transmembrane receptor kinase activity. Genes Dev. 18:2545-2556.
Germain, H., Qu, N., Cheng, Y. T., Lee, E., Huang, Y., Dong, O. X., Gannon, P., Huang, S., Ding, P., Li, Y., Sack, F., Zhang, Y., and Li, X. 2010. MOS11: A new component in the mRNA export pathway. PLoS Genet. 6:e1001250.
Germain, H., and Séguin, A. 2011. Innate immunity: Has poplar made its BED? New Phytol. 189:678-687.
Gloggnitzer, J., Akimcheva, S., Srinivasan, A., Kusenda, B., Riehs, N., Stampfl, H., Bautor, J., Dekrout, B., Jonak, C., Jiménez-Gómez, J. M., Parker, J. E., and Riha, K. 2014. Nonsense-mediated mRNA decay modulates immune receptor levels to regulate plant antibacterial defense. Cell Host Microbe 16:376-390.
Han, T. W., Kato, M., Xie, S., Wu, L. C., Mirzaei, H., Pei, J., Chen, M., Xie, Y., Allen, J., Xiao, G., and McKnight, S. L. 2012. Cell-free formation of RNA granules: Bound RNAs identify features and components of cellular assemblies. Cell 149:768-779.
Johnson, K. C. M., Dong, O. X., Huang, Y., and Li, X. 2013. A rolling stone gathers no moss, but resistant plants must gather their MOSes. Cold Spring Harb. Symp. Quant. Biol. 77:259-268.
Jones, J. D. G., and Dangl, J. L. 2006. The plant immune system. Nature 444:323-329.
Katahira, J. 2012. mRNA export and the TREX complex. Biochim. Biophys. Acta 1819:507-513.
Kubo, M., Furuta, K., Demura, T., Fukuda, H., Liu, Y. G., Shibata, D., and Kakimoto, T. 2011. The *CKH1*/*EER4* gene encoding a TAF12-like protein negatively regulates cytokinin sensitivity in *Arabidopsis thaliana*. Plant Cell Physiol. 52:629-637.
Kulkarni, M., Ozgur, S., and Stoecklin, G. 2010. On track with p-bodies. Biochem. Soc. Trans. 38:242-251.
Lago, C., Clerici, E., Mizzi, L., Colombo, L., and Kater, M. M. 2004. TBP-associated factors in *Arabidopsis*. Gene 342:231-241.
Leaw, C. L., Ren, E. C., and Choong, M. L. 2004. Hcc-1 is a novel component of the nuclear matrix with growth inhibitory function. Cell. Mol. Life Sci. 61:2264-2273.
Leichter, M., Marko, M., Ganou, V., Patrinou-Georgoula, M., Tora, L., and Guialis, A. 2011. A fraction of the transcription factor TAF15 participates in interactions with a subset of the spliceosomal U1 snRNP complex. Biochim. Biophys. Acta 1814:1812-1824.
Li, X., Clarke, J. D., Zhang, Y., and Dong, X. 2001. Activation of an EDS1-mediated R-gene pathway in the snc1 mutant leads to constitutive, NPR1-independent pathogen resistance. Mol. Plant-Microbe Interact 14:1131-1139.
Li, X., Kapos, P., and Zhang, Y. 2015. NLRs in plants. Curr. Opin. Immunol. 32:114-121.
Li, X., Zhang, Y., Clarke, J. D., Li, Y., and Dong, X. 1999. Identification and cloning of a negative regulator of systemic acquired resistance, SNI1, through a screen for suppressors of npr1-1. Cell 98:329-339.
Li, Y., Li, S., Bi, D., Cheng, Y. T., Li, X., and Zhang, Y. 2010. SRFR1 negatively regulates plant NB-LRR resistance protein accumulation to prevent autoimmunity. PLoS Pathog. 6:e1001111.
Liu, J., Rivas, F. V., Wohlschlegel, J., Yates, J. R., 3rd, Parker, R., and Hannon, G. J. 2005. A role for the P-body component GW182 in microRNA function. Nat. Cell Biol. 7:1261-1266.
Lu, D., Wu, S., Gao, X., Zhang, Y., Shan, L., and He, P. 2010. A receptor-like cytoplasmic kinase, BIK1, associates with a flagellin receptor complex to initiate plant innate immunity. Proc. Natl. Acad. Sci. U.S.A. 107:496-501.
Ma, X., Nicole, M. C., Meteignier, L. V., Hong, N., Wang, G., and Moffett, P. 2015. Different roles for RNA silencing and RNA processing components in virus recovery and virus-induced gene silencing in plants. J. Exp. Bot. 66:919-932.
Marko, M., Vlassis, A., Guialis, A., and Leichter, M. 2012. Domains involved in TAF15 subcellular localisation: Dependence on cell type and ongoing transcription. Gene 506:331-338.
Meissner, M., Lopato, S., Gotzmann, J., Sauermann, G., and Barta, A. 2003. Proto-oncoprotein TLS/FUS is associated to the nuclear matrix and complexed with splicing factors PTB, SRm160, and SR proteins. Exp. Cell Res. 283:184-195.
Mireault, C., Paris, L.-E., and Germain, H. 2014. Enhancement of the *Arabidopsis* floral dip method with XIAMETER OFX-0309 as alternative to Silwet L-77 surfactant. Botany 92:523-525.
Mizzen, C. A., Yang, X. J., Kokubo, T., Brownell, J. E., Bannister, A. J., Owen-Hughes, T., Workman, J., Wang, L., Berger, S. L., Kouzarides, T., Nakatani, Y., and Allis, C. D. 1996. The $TAF_{II}250$ subunit of TFIID has histone acetyltransferase activity. Cell 87:1261-1270.
Monaghan, J., Germain, H., Weihmann, T., and Li, X. 2010. Dissecting plant defense signal transduction: Modifier of *snc1* in *Arabidopsis*. Can. J. Plant Pathol. 32:35-42.
Nathans, R., Chu, C. Y., Serquina, A. K., Lu, C. C., Cao, H., and Rana, T. M. 2009. Cellular microRNA and p bodies modulate host-HIV-1 interactions. Mol. Cell 34:696-709.
Ozgur, S., Chekulaeva, M., and Stoecklin, G. 2010. Human Pat1b connects deadenylation with mRNA decapping and controls the assembly of processing bodies. Mol. Cell. Biol. 30:4308-4323.
Palma, K., Zhang, Y., and Li, X. 2005. An importin alpha homolog, MOS6, plays an important role in plant innate immunity. Curr. Biol. 15: 1129-1135.
Parry, G., Ward, S., Cernac, A., Dharmasiri, S., and Estelle, M. 2006. The *Arabidopsis* SUPPRESSOR OF AUXIN RESISTANCE proteins are nucleoporins with an important role in hormone signaling and development. Plant Cell 18:1590-1603.
Pham, A. D., and Sauer, F. 2000. Ubiquitin-activating/conjugating activity of $TAF_{II}250$, a mediator of activation of gene expression in *Drosophila*. Science 289:2357-2360.
Rairdan, G., and Moffett, P. 2007. Brothers in arms? Common and contrasting themes in pathogen perception by plant NB-LRR and animal NACHT-LRR proteins. Microbes Infect. 9:677-686.

Riehs-Kearnan, N., Gloggnitzer, J., Dekrout, B., Jonak, C., and Riha, K. 2012. Aberrant growth and lethality of *Arabidopsis* deficient in nonsense-mediated RNA decay factors is caused by autoimmune-like response. Nucleic Acids Res. 40:5615-5624.

Roux, M. E., Rasmussen, M. W., Palma, K., Lolle, S., Regué, A. M., Bethke, G., Glazebrook, J., Zhang, W., Sieburth, L., Larsen, M. R., Mundy, J., and Petersen, M. 2015. The mRNA decay factor PAT1 functions in a pathway including MAP kinase 4 and immune receptor SUMM2. EMBO (Eur. Mol. Biol. Organ.) J. 34:593-608.

Sugiura, T., Sakurai, K., and Nagano, Y. 2007. Intracellular characterization of DDX39, a novel growth-associated RNA helicase. Exp. Cell Res. 313: 782-790.

Trujillo, M., Ichimura, K., Casais, C., and Shirasu, K. 2008. Negative regulation of PAMP-triggered immunity by an E3 ubiquitin ligase triplet in *Arabidopsis*. Curr. Biol. 18:1396-1401.

Uhrig, J. F., Canto, T., Marshall, D., and MacFarlane, S. A. 2004. Relocalization of nuclear ALY proteins to the cytoplasm by the tomato bushy stunt virus P19 pathogenicity protein. Plant Physiol. 135:2411-2423.

Wiermer, M., Cheng, Y. T., Imkampe, J., Li, M., Wang, D., Lipka, V., and Li, X. 2012. Putative members of the Arabidopsis Nup107-160 nuclear pore sub-complex contribute to pathogen defense. Plant J. 70: 796-808.

Winter, D., Vinegar, B., Nahal, H., Ammar, R., Wilson, G. V., and Provart, N. J. 2007. An "Electronic Fluorescent Pictograph" browser for exploring and analyzing large-scale biological data sets. PLoS One 2: e718.

Xiang, T., Zong, N., Zou, Y., Wu, Y., Zhang, J., Xing, W., Li, Y., Tang, X., Zhu, L., Chai, J., and Zhou, J. M. 2008. *Pseudomonas syringae* effector AvrPto blocks innate immunity by targeting receptor kinases. Curr. Biol. 18:74-80.

Xu, J., and Chua, N. H. 2009. *Arabidopsis* decapping 5 is required for mRNA decapping, P-body formation, and translational repression during postembryonic development. Plant Cell 21:3270-3279.

Xu, J., Yang, J. Y., Niu, Q. W., and Chua, N. H. 2006. *Arabidopsis* DCP2, DCP1, and VARICOSE form a decapping complex required for postembryonic development. Plant Cell 18:3386-3398.

Zhai, J., Jeong, D. H., De Paoli, E., Park, S., Rosen, B. D., Li, Y., González, A. J., Yan, Z., Kitto, S. L., Grusak, M. A., Jackson, S. A., Stacey, G., Cook, D. R., Green, P. J., Sherrier, D. J., and Meyers, B. C. 2011. MicroRNAs as master regulators of the plant NB-LRR defense gene family via the production of phased, trans-acting siRNAs. Genes Dev. 25:2540-2553.

Zhang, Y., Goritschnig, S., Dong, X., and Li, X. 2003. A gain-of-function mutation in a plant disease resistance gene leads to constitutive activation of downstream signal transduction pathways in *suppressor of npr1-1*, *constitutive 1*. Plant Cell 15:2636-2646.

Zhang, Y., and Li, X. 2005. A putative nucleoporin 96 Is required for both basal defense and constitutive resistance responses mediated by *suppressor of npr1-1,constitutive 1*. Plant Cell 17:1306-1316.

Zhang, Z., Wu, Y., Gao, M., Zhang, J., Kong, Q., Liu, Y., Ba, H., Zhou, J., and Zhang, Y. 2012. Disruption of PAMP-induced MAP kinase cascade by a *Pseudomonas syringae* effector activates plant immunity mediated by the NB-LRR protein SUMM2. Cell Host Microbe 11:253-263.

Zipfel, C. 2008. Pattern-recognition receptors in plant innate immunity. Curr. Opin. Immunol. 20:10-16.

AUTHOR-RECOMMENDED INTERNET RESOURCES

WoLF PSORT prediction tool: http://www.genscript.com/wolf-psort.html

National Center for Biotechnology Information Conserved Domain search tool: http://www.ncbi.nlm.nih.gov/Structure/cdd/wrpsb.cgi